Journal of Hazardous Materials 496 (2025) 139299

Contents lists available at ScienceDirect

Journal of Hazardous Materials

journal homepage: www.elsevier.com/locate/jhazmat

Microbial degradation of two major phytotoxic alkaloids from barley

Yanfei Wu, Tao Li *, Ning-Yi Zhou *

State Key Laboratory of Microbial Metabolism, Joint International Research Laboratory of Metabolic and Developmental Sciences, and School of Life Sciences and Biotechnology, Shanghai Jiao Tong University, Shanghai 200240, China

HIGHLIGHTS

- Two isolated bacteria can degrade the phytotoxic alkaloids hordenine and gramine.
- Three metabolites were identified as key products of the alkaloids' degradation.
- Genomic analysis revealed gene clusters associated with the degradation pathways.
- Bacterial degradation pathways for hordenine and gramine have been proposed.

GRAPHICAL ABSTRACT

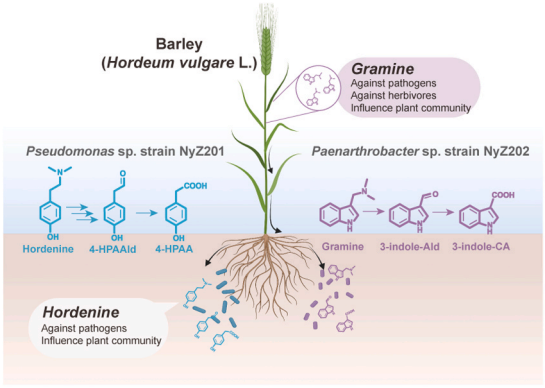

ARTICLE INFO

Keywords:
Barley alkaloids
Biodegradation
Gramine
Hordenine
Rhizospheric microorganism

ABSTRACT

Barley (*Hordeum vulgare* L.) produces phytotoxic alkaloids hordenine and gramine as defense compounds against pests and pathogens. These alkaloids also influence rhizosphere microbial communities, and their persistence in soil poses potential ecological risks due to their phytotoxicity. However, the microorganisms and pathways involved in their degradation have not yet been characterized. Here, a Gram-negative bacterium (*Pseudomonas* sp. strain NyZ201) and a Gram-positive bacterium (*Paenarthrobacter* sp. strain NyZ202) were successfully isolated from barley rhizosphere for their respective evident growth with hordenine (doubling time = 2.5 h) and gramine (doubling time = 3.8 h) as sole sources of carbon, nitrogen and energy. High-resolution mass spectrometry and ^{18}O-labeling experiments identified key catabolic intermediates formed by hydrolysis or dehydrogenation. Through whole-genome sequencing analysis, we proposed degradation pathways for these two barley alkaloids and predicted the associated gene clusters harbored by these strains. These findings offer novel insights into the microbial degradation of phytotoxic alkaloids from barley, and provide a basis for the detoxification of phytotoxic alkaloids in agricultural ecosystems.

* Corresponding authors.
E-mail addresses: yf.wu1@sjtu.edu.cn (Y. Wu), lisuitao@sjtu.edu.cn (T. Li), ningyi.zhou@sjtu.edu.cn (N.-Y. Zhou).

https://doi.org/10.1016/j.jhazmat.2025.139299
Received 16 May 2025; Received in revised form 14 July 2025; Accepted 16 July 2025
Available online 17 July 2025

1. Introduction

Plants produce a vast array of phytotoxic compounds that are integral to their interactions with the environment, including defense, communication, and adaptation [1,2]. Plant releases toxic compounds (e.g., alkaloids, terpenes, phenylpropanoids, aristolochic acids) into soil ecosystems, potentially forming organic micropollutants that impact agricultural ecosystems and human health [3,4]. The environmental persistence and transformation pathways of these compounds remain poorly characterized despite their demonstrated adverse effects in the environment. This knowledge gap hinders the evaluation of their ecological risks through microbial transformation or potential accumulation in soil ecosystems.

Alkaloids are a large group of nitrogen-containing compounds that are potentially toxic plant secondary metabolites, including nicotine [5], and benzoxazinoids [6,7], which exhibit extremely various chemical structures and diverse biological activities [1,8]. Among them, hordenine (a phenylethylamine alkaloid) and gramine (an indole methylamine alkaloid) are of great interests due to being the major allelopathic alkaloids exuding by various species of Gramineae and Leguminosae, particularly the widely cultivated cereal crop barley (*Hordeum vulgare* L.) [9–12]. Both hordenine and gramine belong to aromatic alkaloids containing the methylamine group, but different precursors and pathways are employed for their biosynthesis in plants [13]. Biosynthesis pathway of hordenine has been well elucidated, which is derived from the tyrosine [14,15]. In contrast, biosynthesis of gramine from tryptophan has been recently revealed in barley, which involves an extraordinary oxidative rearrangement process [16,17]. Barley produced hordenine (327μg/g dry weight) in roots and gramine (8 mg/g dry weight) in shoots [13]. These two alkaloid compounds display a variety of biological activities and phytotoxic potential, encompassing insecticidal effects and plant defense responses [18–23]. Notably, gramine demonstrates toxicity to plants, animals, bacteria and fungi, as reported in numerous studies [24–27].

Meantime, hordenine and gramine also display various influences on rhizospheric microbiota and agricultural soil ecosystem [28,29]. Hordenine was found to function as a bacterial quorum sensing inhibitor and disrupt the formation of biofilm [30]. Its structural analog gramine can modulate the assembly of rhizospheric microbiota and shape the microbiota [29]. Especially, gramine seems to play a crucial role on the recruitment of a subset of soil beneficial microbes [31]. However, the underlying mechanism for this effect of gramine is elusive at present, whereas the degradation of gramine by resident microbes in the rhizosphere is supposed to be an influence factor [31]. On the other hand, gramine exhibits mammalian toxicity [25] and negatively affects its usability as fodder due to its ruminant antifeedant properties [26]. It is understood that the catabolic fate of hordenine and gramine would significantly impact their persistence in soil ecosystem. Biodegradation and biotransformation represent sustainable, cost-effective alternative methods for environmental remediation of widespread and trace pollutants [32]. Nevertheless, while the microbial degradation of the hordenine and gramine analogs, such as tyrosine[33], tyramine[34], tryptophan[35], and 3-indole acetic acid [36,37], has been extensively studied, microbial degradation of hordenine and gramine remains enigmatic. Therefore, understanding the degradation pathways of these plant-produced alkaloids by rhizospheric microorganisms would be beneficial for revealing their roles in shaping the rhizosphere microbiome and supporting environmentally sustainable agricultural management [11,38,39].

Here, we described the successful isolation of two bacterial strains from barley rhizosphere soil that are capable of utilizing hordenine or gramine as sole source of carbon, nitrogen and energy for growth. Distinct catabolism pathways for hordenine and gramine were proposed based on the results of intermediate identification, isotope labeling experiment, and whole genome sequencing analysis. Our findings will provide an opportunity to gain biochemical insights into how bacteria catabolize the phytotoxic alkaloids hordenine and gramine.

2. Materials and methods

2.1. Bacterial strains and culture conditions

Mineral salts medium (MSM) containing 1or 2 mM hordenine or gramine was used for the growth of corresponding degraders. Nitrogen-free MSM consisted of (per liter) 3 g KH_2PO_4, 14.3 g $Na_2HPO_4{\cdot}12\ H_2O$, 0.28 mg $MnSO_4{\cdot}H_2O$, 1.0 mg $CaCl_2$, 0.05 mg $CuSO_4$, 0.05 mg $ZnSO_4$, 0.30 mg $FeSO_4{\cdot}7\ H_2O$ and 0.06 mg $MgSO_4{\cdot}7\ H_2O$. MSM was supplemented with 0.2 % (w/v) ammonium sulfate as a nitrogen source when necessary. Lysogeny broth (LB) medium comprised the following components (per liter): 10.0 g tryptone, 10.0 g NaCl, and 5.0 g yeast extract. Tryptone soy broth (TSB) medium comprised 30.0 g tryptone soy broth (per liter) and 1/5 strength TSB were used throughout the work. Agar media of MSM, LB and TSB were prepared by adding 1.5 % (wt/vol) agar powder.

2.2. Isolation and identification of hordenine and gramine degrading bacteria

Hordenine and gramine degrading bacteria were isolated from barley rhizosphere soil collected from fields in Henan Province, China. Soil samples were suspended in sterile MSM. Selective enrichment was achieved by inoculating these suspensions into MSM supplemented with 1 mM hordenine or 1 mM gramine, respectively. Incubations were conducted at 30 °C with shaking at 180 rpm for two weeks. Subsequently, serial transfers to fresh MSM containing 1 mM of the respective substrate were performed thrice to ensure enrichment efficacy as previously described [40]. Following three rounds of enrichment, cultures were diluted and plated onto TSB agar plates for isolation of single colonies. Candidate isolates were then subjected to growth assay in MSM supplemented with 2 mM hordenine or gramine. Taxonomic identification was based on morphological characteristics using a TESCAN high-resolution scanning electron microscope (SEM) operating at 10 kV, and sequence alignment of 16S rRNA gene (see below).

2.3. Bacterial degradation of hordenine and gramine

Hordenine utilizer *Pseudomonas* sp. strain NyZ201 and gramine utilizer *Paenarthrobacter* sp. strain NyZ202 were pre-grown overnight in MSM supplemented with 2 mM hordenine and 2 mM gramine, respectively, on a rotary shaker (30°C, 180 rpm). These overnight cultures were then used to inoculate fresh MSM (1 % inoculum) containing 2 mM hordenine and 2 mM gramine, respectively. During the biodegradation process, bacterial growth was represented by the optical density at 600 nm (OD_{600}), and substrates depletion were monitored throughout using high-performance liquid chromatography (HPLC).

To understand whether the alkaloids degradation by these strains is inducible or constitutive, separate cultures of each strain were pre-grown in MSM supplemented with 2 mM sodium succinate, 2 mM hordenine (for strain NyZ201) or gramine (for strain NyZ202). A 1 % inoculum was then transferred to fresh MSM containing either 2 mM sodium succinate as an untreated control and 2 mM hordenine or gramine as a treatment sample. The cells were harvested when reaching their stationary phase ($OD_{600}\approx0.12$ for strain NyZ201, $OD_{600}\approx0.18$ for strain NyZ202) of growth (30 °C, 180 rpm), and then washed with 100 mM PBS (pH 7.4). The whole cell biotransformation was prepared using cells at an $OD_{600}\approx$ 0.1, along with 2 mM respective substrate in 10 mL of PBS buffer (pH 7.4). Samples were collected at regular intervals, and substrate concentrations were quantified using HPLC. Each experimental setup was conducted in triplicate.

2.4. Growth substrates test

The growth of strains NyZ201 and NyZ202 on several proposed intermediates was assessed using MSM supplemented with 2 mM of each compound. For NyZ201, the intermediates tested were tyramine, 4-HPAA, N-methyl-tyramine, methylamine, trimethylamine and dimethylamine. For strain NyZ202, the intermediates tested were 3-indoleacetic acid (3-indole-AA), 3-indole-carboxaldehyde (3-indole-Ald), 3-indole-carboxylic acid (3-indole-CA), 4-aminomethylindole, tyramine, methylamine, trimethylamine and dimethylamine. Growth was monitored by measuring the increase of OD_{600} value using an automatic microbial growth analyzer (Bioscreen C MBR). A 1 % inoculum was used in each case with three replicates.

2.5. Isotope labeling experiment

The strains were inoculated into 10 mL of MSM containing 2 mM hordenine or 2 mM gramine and grown until reaching the stationary phase at temperature of 30°C (OD_{600}≈0.12 for strain NyZ201, OD_{600}≈0.18 for strain NyZ202). Subsequently, cells were harvested by centrifugation (12,000 ×g, 10 min, 4°C). The harvested cells were divided into two equal volumes, with one volume being washed twice with 100 mM PBS (pH 7.4) dissolved in $H_2^{18}O$ and the other volume being washed twice with 100 mM PBS buffer (pH 7.4) dissolved in H_2O. Each reaction mixture (0.4 mL total volume) contained 2 mM substrate, washed cells (OD_{600}≈1.5 for strain NyZ201; OD_{600}≈2.2 for strain NyZ202), and either 100 mM isotope labeled or unisotope labeled PBS (pH 7.4). These mixtures were then incubated at 30°C for 2 h, before the reaction was terminated by centrifuging (12,000 ×g, 10 min) and to collect the supernatant, where the possible intermediates from above biotransformation were analyzed by ultra-high performance liquid chromatography (UPLC, Agilent 1290 Infinity II) coupled with a high-resolution mass spectrometer (HRMS, Agilent 6546 Q-TOF).

2.6. 16S rRNA gene sequencing

Genomic DNA was extracted from NyZ201 and NyZ202 cells using a bacterial DNA isolation Kit (OMEGA Biotek, China). The 16S rRNA gene was amplified via polymerase chain reaction (PCR) using forward primer 27 F (5′-AGAGTTTGATCCTGGCTCAG-3′) and reverse primer 1492 R (5′-TACGGCTACCTTGTTACGACTT-3′) as previously described [41], and the amplicons were sequenced by Tsingke Bio Co., Ltd (Beijing, China). The resultant 16S rRNA gene sequences (GenBank accession numbers: PV195285 for strain NyZ201, and PV195287 for strain NyZ202) were analyzed using NCBI BLAST [42] and EzBioCloud database[43] to identify homologous sequences. Phylogenetic tree was constructed using MEGAX software[44] with the maximum likelihood method.

2.7. Whole genome sequencing

Whole-genome sequencing of strains NyZ201 and NyZ202 was performed by Personalbio Co., Ltd (Shanghai, China). The raw data generated from PacBio Sequel IIe and Illumina platform were assembled into consensus sequences, then processing for circularization and resulting in a closed genome sequence. Protein-coding sequences (CDSs) were predicted from the closed genomes and functionally annotated against the NR and KEGG databases using Diamond [45] with homology-based cutoff criteria of E-value < 1e-6. Biosynthetic gene clusters (BGCs) encoding the synthesis of secondary metabolites were identified with antiSMASH v5.1.2 software [46]. The CGView was employed for genome visualization and analysis [47]. Average nucleotide identity (ANI) values were calculated via tetra correlation search in JSpeciesWS [48]. The general information of the genomes are shown in Table S1. The complete genome sequences of strains NyZ201 and NyZ202 have been deposited in the NCBI database under accession numbers CP187557 and CP187556, respectively.

2.8. Analytical methods

Quantitation of substrates and biotransformation intermediates was performed by HPLC (Agilent 1260 Infinity II) using an Agilent ZORBAX SB-C18 column (5 μm, 4.6 ×250 mm). The mobile phase consisted of water containing 0.1 % (v/v) formic acid (A) and acetonitrile (B), with gradient elution: 0–2 min 5 % B; 2–10 min 5 %-100 % B; 10.0–10.1 min 100 %-5 % B; 10.1–11 min 5 % B. The flow rate was 1 mL/min, the column temperature was set as room temperature, the injection volume was 5 μL, and detection wavelength was 278 nm.

Intermediates were identified by UPLC-HRMS using the same mobile phase as HPLC but with a modified elution gradient: 0–4 min 5 % B;4–16 min 5 %-100 % B;16–20 min 95 %-5 % B. The DAD recorded spectra from 200 to 400 nm. The injection volume was 5 μL and the flow rate was 0.4 mL/min. Mass spectrometer was used with the following parameters: sheath gas flow, 11 L/min; the sheath gas temperature, 350°C; nebulizer pressure, 35 psi; drying gas flow, 8 L/min, VCap, 4000 V; nozzle voltage, 200 V; fragmentor, 90 V; skimmer, 65 V, 100–1700 *m/z* mass range, electrospray ionization source (ESI). Both positive and negative ion modes were used for detection.

2.9. Statistical analysis

Origin 2019 and Microsoft Excel 2021 software were utilized for the statistical analysis. All quantitative data were expressed as standard deviation (SD).

3. Results and discussion

3.1. Isolation of Barley alkaloids utilizing bacteria

To isolate possible rhizobacteria that is capable of degrading major barley alkaloids hordenine and gramine, root-surface soil samples were collected from a barley field in Henan Province (China). After enrichment procedures, two strains degrading hordenine and gramine respectively were obtained (Figure S1A). The colonies of one strain showing hordenine degradation capacity were grayish-white, semi-transparent, smooth, central protrusion, and round shape when grown on TSB agar plates (Figure S1A-1). SEM analysis revealed rod-shaped cells approximately 1.5 μm in length and 0.4 μm in width, with a wrinkled surface (Figure S1A-2). The colonies of other strain showing gramine degradation capacity were similar to hordenine-degrader in colony morphotype, but with light yellow in color (Figure S1A-3). SEM analysis showed smooth, short rod-shaped cells (Figure S1A-4).

Phylogenetic analysis based on 16S rRNA gene sequences indicated that the hordenine degrader is closely related to the *Pseudomonas bharatica* CSV86^T [49], a recognized aromatic compounds utilizer (Figure S1B). Whole-genome comparative analysis (see below) further clarified its taxonomic position through average nucleotide identity (ANI) calculations (Tables S2). This strain exhibited ANIb and ANIm values of 96.34 % and 97.51 %, respectively, against *Pseudomonas bharatica* CSV86^T [49], while showing higher nucleotide identities (ANIb: 98.59 %; ANIm: 98.91 %) with *Pseudomonas putida* CBF10–2 [50]. However, definitive species assignment could not be precluded from the ambiguous clustering with these two strains. Consequently, the strain was designated *Pseudomonas* sp. strain NyZ201. Members of the *Pseudomonas* species are renowned for their catabolic versatility, including documented catabolic capabilities toward biogenic amines [51].

Phylogenetic analysis based on 16S rRNA gene sequences placed gramine degrader within the *Paenarthrobacter* clade (98.7 % 16S rRNA identity to *Paenarthrobacter ilicis* DSM 20138) which showed divergence from *Arthrobacter* relatives (Figure S1C). Genomic analysis revealed that the strain exhibited closest relatedness to *Paenarthrobacter nicotinovorans*

JCM 3874 [52] (ANIb: 80.38 %; ANIm: 86.18 %), which is lower than the species delineation threshold (Table S3). Combined phylogenetic and genomic evidence suggests this strain as a probable novel species, tentatively designated *Paenarthrobacter* sp. strain NyZ202. The high 16S rRNA gene sequence identity but low whole-genome level identity implied that frequent horizontal gene transfer may have occurred in the genome of strain NyZ202.

3.2. Barley alkaloids degradation by newly isolated two bacterial strains

Strains NyZ201 and NyZ202 exhibited efficient degradation capacities toward hordenine and gramine, respectively. When growing on MSM supplemented with 2 mM hordenine, strain NyZ201 displayed an evident exponential growth following a12-hour lag phase, and reaching a maximum OD_{600} value of 0.12 at 22 h. The rapid degradation of hordenine was observed during the exponential growth period of strain NyZ201 (Fig 1A1). Then the bacterial growth entered the stationary phase accompanying by hordenine exhaustion. On the other hand, gramine-grown NyZ202 cells exhibited a 20-hour lag phase and reached a maximum OD_{600} value of 0.2 at 28 h with gramine exhaustion (Fig 1B1). As for the two control groups, the substrate concentration remained unchanged without bacterial inoculation, and no increase in the bacterial biomass without the addition of the substrates, indicating that substrates degradation was entirely attributed to the bacterial catabolism. No growth was observed for strain NyZ201 on gramine, and vice versa.

In the whole cell biotransformation assays, pretreatment of strains NyZ201 or NyZ202 cells with their respective substrates (hordenine or gramine) significantly enhanced the degradation rates compared to their succinate-grown cells. Specifically, hordenine-grown NyZ201 cells exhibited a degradation rate of 64.7 μM/min/OD_{600} to hordenine (Fig 1A2). Meanwhile, a UV–visible intermediate (λ_{max}=275 nm) was observed during the degradation process of hordenine, and lately identified to be 4-hydroxyphenylacetic acid (4-HPAA) (see below for intermediates identification). In regard to gramine, it was degraded by gramine-grown NyZ202 cells at rate of 37.3 μM/min/OD_{600} (Fig 1B2), from which two intermediates 3-indole-Ald and 3-indole-CA were identified (see below for intermediates identification). The 3-indole-Ald gradually accumulated to a maximum concentration at approximately 1 h. Subsequently, 3-indole-Ald concentration started to decrease, accompanying with the increased accumulation of 3-indole-CA. This transformation pattern implied that the transient intermediate 3-indole-Ald from gramine was being gradually converted into 3-indole-CA (Fig 1B2). The concentration of both hordenine and gramine remained virtually unchanged when transforming with the succinate-cells (Fig. 1A2&B2). Overall, these results strongly suggest that the catabolic pathways for both hordenine and gramine are inducible in these two strains, which would be helpful to identify the genes involved by differential transcriptomics.

The influence of environmental conditions on the degradation

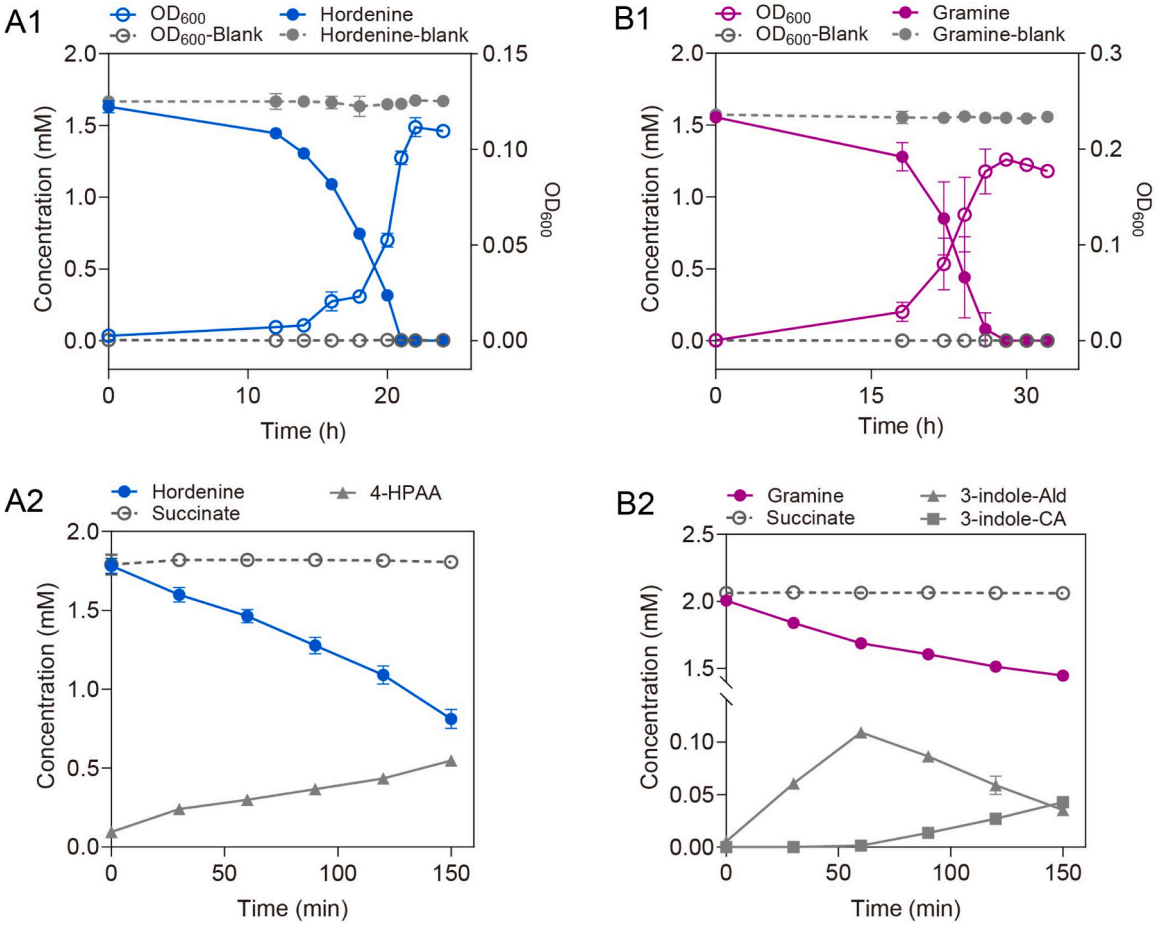

Fig. 1. Degradation of barely alkaloids by strains NyZ201 and NyZ202. (A1) Growth of strain NyZ201 on hordenine as sole carbon and nitrogen source. (A2) Degradation of hordenine by the strain NyZ201 cells grown on succinate or hordenine. Cells were cultivated in minimal salts medium containing 2 mM succinate or hordenine, the cells were harvested and suspended to OD_{600} value of 1.5. The degradation of ~2 mM hordenine by the succinate or hordenine-grown cells was performed at 30°C and samples were taken at designated timepoints. 4-HPAA: 4-hydroxyphenylacetic acid. (B1) Growth of strain NyZ202 on gramine as sole carbon and nitrogen source. (B2) Degradation of gramine by the strain NyZ202 cells grown on succinate or gramine as the method described in A2. Data points represent the mean of three independent replicates.

efficiency of both strains was investigated by evaluating their performance across varying pH and temperature conditions. The degradation results showed that strain NyZ201 exhibits maximal hordenine degradation at pH 7.0 and 30°C (Figure S2A). Strain NyZ202 exhibits maximal gramine degradation at pH 9.0 and 30 °C, indicating a greater suitability for slightly alkaline conditions (Figure S2B). The strain NyZ202 alkaline tolerance may be advantageous in environments such as alkaline soils. Both strains remain functional across a broad pH range (4.0–10.0) and temperature range (4–40 °C), demonstrating robust environmental adaptability for potential applications.

3.3. *Identification of intermediates during hordenine degradation by strain NyZ201*

Having phenotypically characterized barely alkaloids-degrading strains, we were curious about the catabolic fate of hordenine and gramine by the Gram-negative strain NyZ201 and Gram-positive strain NyZ202, respectively. In order to capture intermediates from the degradation of hordenine by strain NyZ201, whole cell biotransformation toward hordenine was performed. Initially, no substantial accumulation of any intermediate was observed during the growth of strain NyZ201 on hordenine as sole carbon and nitrogen source, probably due to its robust metabolic flux (Figures S3A1). However, when the hordenine was transformed by the resting cells of strain NyZ201, the appearance of a major intermediate peak with retention time of 7.8 min coincided with the decrease of hordenine (Retention time=4.7 min; *m/z* 166.1249 $[M+H]^+$) (Figure S3A2). Its UPLC-HRMS produced the molecular formula $C_8H_7O_3$ (*m/z* 151.0402 $[M-H]^-$, mass accuracy: 0.07 parts per million [ppm] error) which was identified to be 4-hydroxyphenylacetic acid (4-HPAA) based on the comparation with authentic 4-HPAA (Fig. 2). In addition, HRMS analyses revealed another intermediate with inferred molecular formulas $C_8H_7O_2$ (*m/z* 135.0452 $[M-H]^-$), which is identical to 4-hydroxyphenylacetaldehyde (4-HPAAld) (Figure S4).

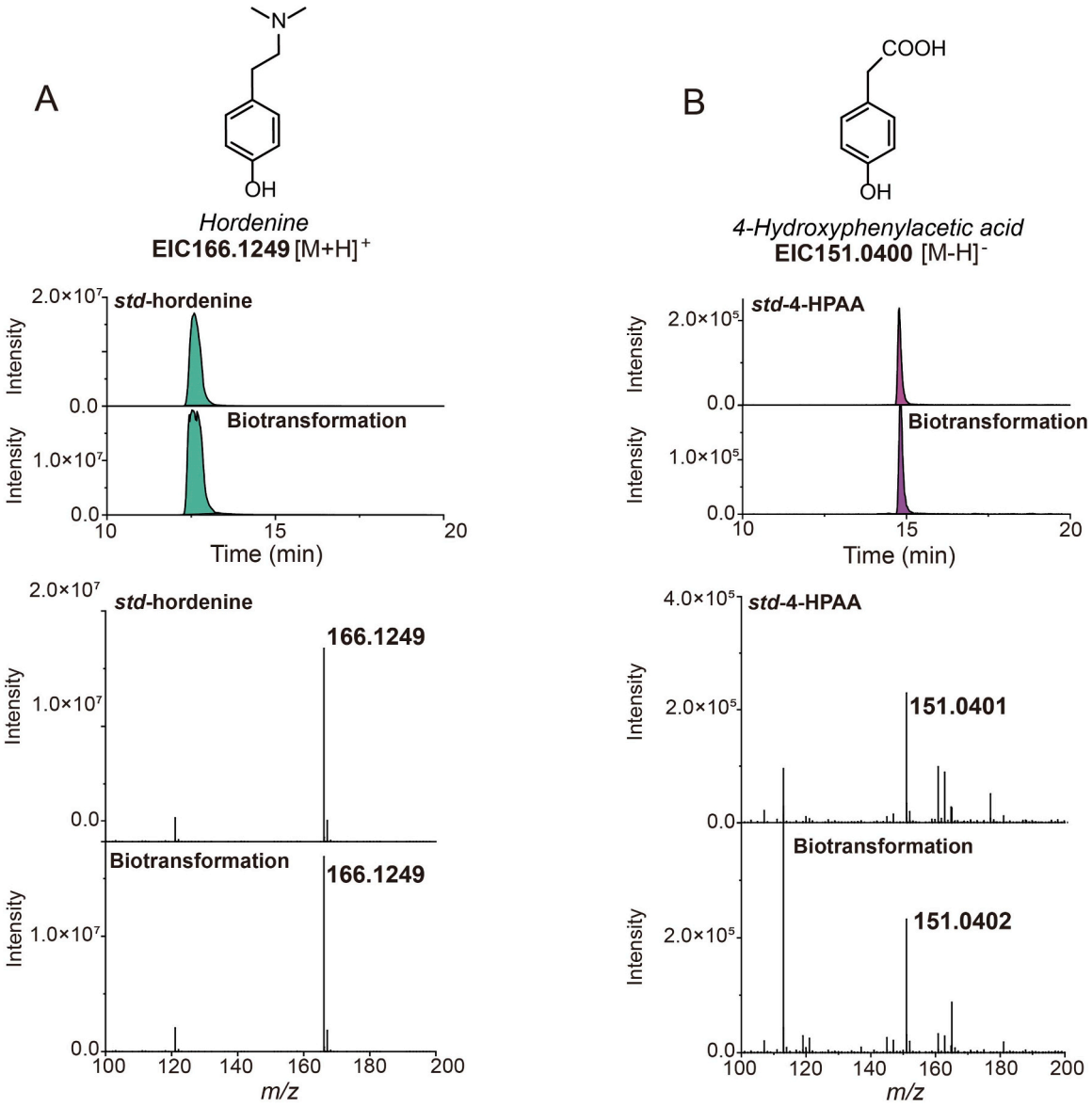

Fig. 2. UPLC–HRMS analysis of hordenine degradation intermediates by strain NyZ201. Degradation intermediates were identified from whole cell biotransformation assays. Extracted ion chromatogram (EIC) peaks are annotated with corresponding compounds and their mass spectra. "Std" denotes the authentic standard. The detected compounds include hordenine (A) and 4-HPAA (B).

3.4. Identification of intermediates during gramine degradation by strain NyZ202

Whole cell biotransformation was also performed to identify the intermediates from the degradation of gramine by strain NyZ202. The identities of the intermediate peaks were assessed by their chromatographic feature and the high-resolution mass spectra (Fig. 3). Gramine (Retention time=7.2 min, *m/z* 175.1241 $[M+H]^+$) was transformed by the NyZ202 cells, coinciding with the increase of a new peak at the retention time of 9.1 min, which was determined to be indole-3-carboxaldehyde (3-idole-Ald, *m/z* 146.0602 $[M+H]^+$, mass accuracy: 0.14 parts per million [ppm] error) (Fig. 3B & S3B). Meanwhile, another peak (Retention time=8.5 min) gradually accumulated since 60 min (Fig. 1B2), and it was consistent with the HPLC chromatogram and mass spectrometry of authentic indole-3-carboxylic acid (3-indole-CA, *m/z* 162.0550 $[M+H]^+$, mass accuracy: 0.00 parts per million [ppm] error) (Fig. 3C & S3B).

3.5. Growth substrates of hordenine utilizer strain NyZ201 and gramine utilizer strain NyZ202

To clarify the catabolic step as well as the downstream pathway, a range of putative intermediates were tested as sole carbon sources for the growth of strains NyZ201 and NyZ202. Growth experiment indicated that strain NyZ201 was able to utilize *N*-methyl-tyramine, tyramine and 4-HPAA (Fig. 4A) whereas could not use methylamine substances (Figure S5A). Strain NyZ201 exhibited similar growth curves to that with hordenine when supplemented with *N*-methyl-tyramine or tyramine. Notably, strain NyZ201 uses 4-HPAA more readily, with a more rapid growth and higher accumulation of biomass than those of other tested substrates even including hordenine. This implied that the transformation of hordenine into 4-HPAA would be a rate limit step during the growth of stain NyZ201 on hordenine.

With regard to NyZ202, the growth on putative intermediates 3-indole-AA, 3-indole-Ald, 3-indole-CA, 4-aminomethylindole, methylamine, trimethylamine, dimethylamine at a concentration of 2 mM were analyzed (Fig. 4B & S5B). Like strain NyZ201, no growth of strain NyZ202 was observed on the methylamine substances (Figure S5B). On the other hand, strain NyZ202 could grow on 3-indole-Ald and 3-indole-CA, two intermediates previously identified by HRMS. In particular, strain NyZ202 exhibited a comparable growth on 3-indole-Ald to that on gramine, but 3-indole-CA was poorly utilized. Considering that the 3-indole-CA is a downstream intermediate when rapid growth of strain NyZ202 on 3-indole-Ald and gramine, it would be reasonable to speculate that the weak growth of strain NyZ202 on 3-indole-CA is probably due to the less efficient transportation of 3-indole-CA.

3.6. Oxygen atoms of intermediates 4-HPAA and 3-indole-CA were incorporated from $H_2^{18}O$

From the results of intermediates identification, the catabolism of both hordenine and gramine evidently included the incorporation of oxygen atom during the initial steps, resulting in the formation of 4-HPAA and 3-indole-CA, respectively. To determine the source of the oxygen atom incorporated into these intermediates and the reaction type, whole cell biotransformation assays were performed in isotope

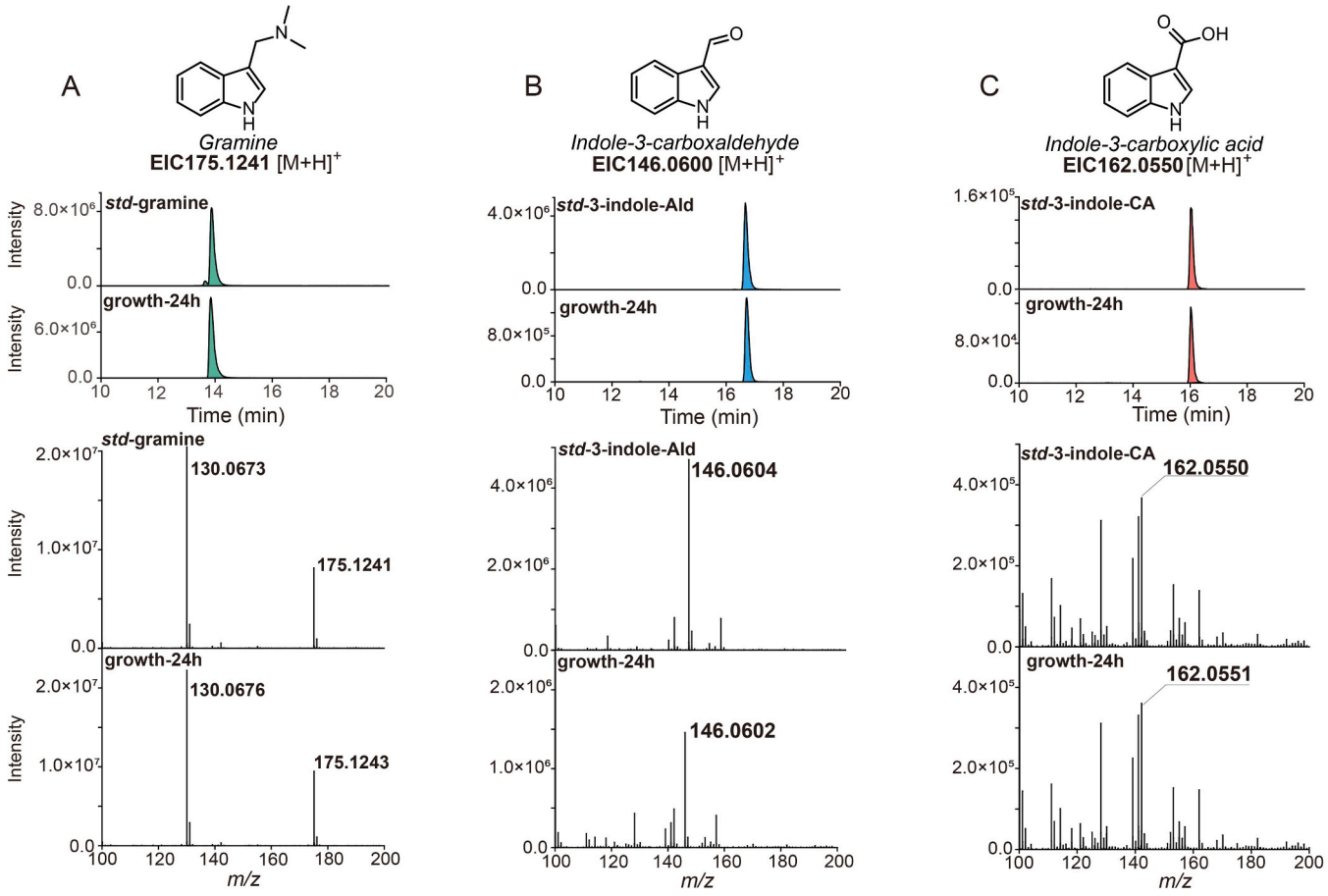

Fig. 3. UPLC–HRMS analysis of gramine degradation intermediates by strain NyZ202. Degradation intermediates were identified from cells growth process. EIC peaks are labeled with corresponding compounds and their mass spectra. "Std" denotes the authentic standard. The detected compounds include gramine (A), 3-indole-Ald (B), 3-indole-CA (C).

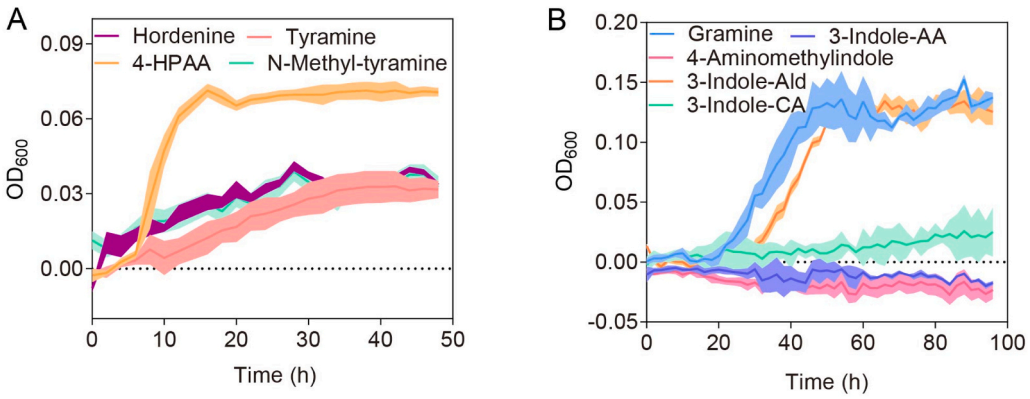

Fig. 4. Growth curves of strain NyZ201 (A) and NyZ202 (B) with proposed intermediates. All data were collected from triplicate experiments, and error bands denote the standard deviation (SD).

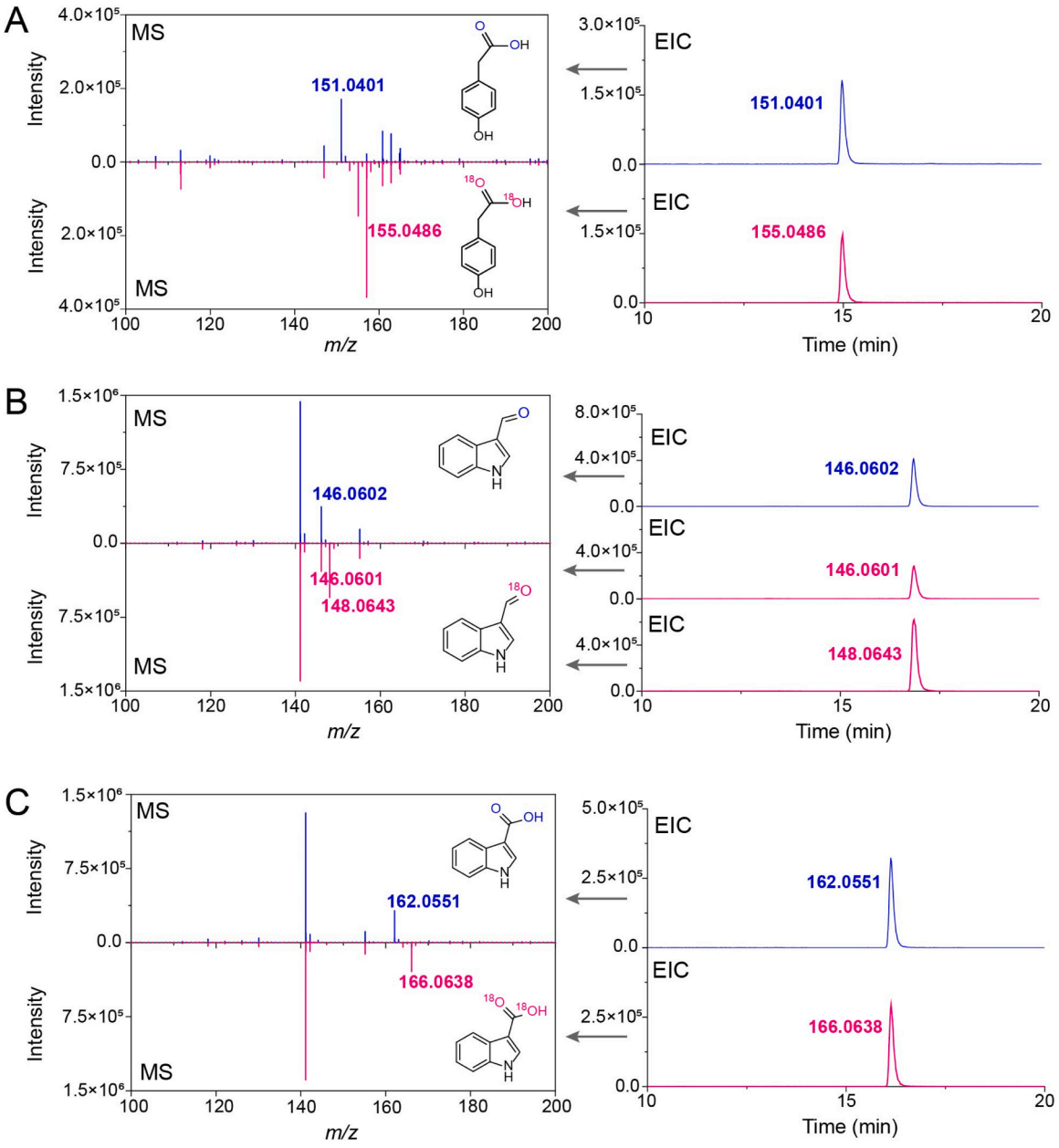

Fig. 5. Isotope labeling experiment. Mass spectra and extracted ion chromatograms for unlabeled isotopes (blue lines) and labeled isotopes (purple lines) are displayed for comparison. The detected intermediates include 4-HPAA (A), 3-indole-Ald (B), 3-indole-CA (C).

labelling $H_2^{18}O$ to covert the substrates into intermediates, which were examined by mass spectrometer. In the hordenine degradation, the molecular ion of ^{18}O atom-labeled 4-HPAA (*m/z* 155.0486) appeared at a position four mass numbers higher than the corresponding ion of unlabeled 4-HPAA (*m/z* 151.0401), indicating the incorporation of two oxygen atoms from H_2O (Fig. 5A). In addition, ^{18}O atom-labeled 3-indole-Ald (*m/z* 148.0643) appeared at position two mass numbers higher than the corresponding ion of unlabeled 3-indole-Ald (*m/z* 146.0602) (Fig. 5B). The observed intermediate of ^{18}O labeled and unlabeled 3-indole-Ald was about 2:1, and this is likely because of the incorporation of H_2O within the cells. During the gramine degradation assay, the molecular ion of ^{18}O atom-labeled 3-indole-CA (*m/z* 166.0638) also appeared at position four mass numbers higher than the corresponding ion of unlabeled 3-indole-CA (*m/z* 162.0551) (Fig. 5C). Thus, the ^{18}O atom of $H_2^{18}O$ was incorporated into 3-indole-Ald and 3-indole-CA, indicating the reactions proceeded via hydrolysis or dehydrogenation.

3.7. Genome analysis of strains NyZ201 and NyZ202

Whole-genome sequencing of strains NyZ201 and NyZ202 was performed to provides molecular understanding of bacterial catabolic pathways for hordenine and gramine. The closed genome of *Pseudomonas* sp. strain NyZ201 is 6.3 Mb with GC content of 64.47 %. It contains 5552 open reading frames (ORFs), 19 rRNA genes, and 71 tRNA genes. While *Paenarthrobacter* sp. strain NyZ202 genome has a total length of 4.5 Mb and a GC content of 63.82 %, with 4142 ORFs, 18 rRNA genes, and 54 tRNA genes. Neither strain carries plasmid. (Figure S6 A1 & B1, Table S1).

Gene annotation and metabolic pathway analyses revealed versatile metabolic expertise for the two strains. KEGG orthology annotation of the genomes assigned a total of 4338 and 1923 genes for strains NyZ201 and NyZ202, respectively, spanning 39 s-level functional categories. Notably, most of the annotated genes of strain NyZ201 (2115) and strain NyZ202 (1617) belong to the metabolism function categories, such as amino acid metabolism, carbohydrate metabolism, cofactor and vitamin metabolism, and energy metabolism. Additionally, a large portion of genes is related to cellular and environmental information processing including cellular community, membrane transport and signal transduction (Figures S7 & S8). Strain NyZ201 exhibits extensive genetic machinery for environmental interactions, including prokaryotic cellular communities (261 genes), membrane transport (263 genes), and signal transduction (349 genes). Coupled with prolific secretion of extracellular flocculent substances, these traits strongly support biofilm formation and quorum sensing, key adaptive strategies for rhizosphere colonization and microbial community modulation [53,54]. In contrast, strain NyZ202 maintained core metabolic functionality while streamlining its genome, preserving critical genes linked to prokaryotic cellular communities (77 genes), membrane transport (151 genes), and signal transduction (95 genes). Both strains exhibited abundant transporters and signaling modules, an indication of heightened environmental responsiveness. These data suggest the potentials for substrate uptake and utilization, metabolic regulation, as well as energy conversion. These traits likely enhance their ability to shape rhizosphere microbial communities through metabolic cross-talk or niche competition, highlighting their ecological adaptability in plant-associated environments.

Moreover, analysis of xenobiotics biodegradation and metabolism pathways revealed that NyZ201 and NyZ202 harbored 170 and 73 genes, respectively, for metabolism of aromatic compounds, suggesting their robust capacity for catabolizing benzoate, aminobenzoate, styrene, naphthalene and etc (Figures S6 A2 & B2). These pathways may also be involved in the degradation of aromatic compounds hordenine and gramine, which are discussed below.

3.8. Proposed pathway for hordenine biodegradation

Through comprehensive analysis of metabolite profiling and isotopic tracer experiments, catabolic pathways for these two barley alkaloids degradation in these strains were revealed. Growth experiments suggest that strain NyZ201 may utilize intermediate *N*-methyl-tyramine, tyramine and 4-HPAA as substrates during hordenine catabolism. Notably, the intermediates 4-HPAAld and 4-HPAA were detected by UPLC-HRMS analysis in this pathway. The hypothesized degradation pathway initiates with *N*-demethylation of hordenine (*N*, *N*-dimethyltyramine), likely catalyzed by a dimethylamine monooxygenase (DmmABC: gene2731–2733) identified through whole-genome annotation (Table S4). This monooxygenation removes one methyl group to generate *N*-methyl-tyramine, followed by complete demethylation to yield tyramine (Fig. 6A). Previous reports on strains *Pseudomonas putida* U [34] and *Escherichia coli* [55] have established a metabolic pathway for tyramine catabolism, where the downstream conversion of tyramine to 4-HPAAld is mediated by a tyramine oxidase encoded by *tyn*AB cluster [34]. Genomic analysis of strain NyZ201 also identified a homologous tyramine oxidase (TynAB: gene2844/gene2842 or gene2536/gene2534), suggesting its potential involvement in tyramine degradation in this strain. Subsequent isotopic tracing experiments using $H_2^{18}O$ labeling provided critical evidence for the fate of the aldehyde intermediate 4-HPAAld to form 4-HPAA, indicating its rapid oxidation by an NAD^+ dependent aldehyde dehydrogenase (TynC: gene3587). A gene cluster (spanning genes3547–3554 and 3585–3586) was found to be homologous to a typical 4-HPAA degradation module (*hpaBCDEFG1G2HI* cluster) in *Pseudomonas putida* U [34] for the canonical pathway. This conserved system mediates an 8-step enzymatic conversion of 4-HPAA to succinate through hydroxylation and ring cleavage reactions. Final integration into central metabolism occurs via succinic semialdehyde dehydrogenase (SSADH: gene3451), completing a 12-enzyme cascade that channels hordenine into the tricarboxylic acid (TCA) cycle as shown in Fig. 6A and Table S4.

3.9. Proposed pathway for gramine biodegradation

As indicated above, growth profiling demonstrated strain NyZ202 was unable to utilize proposed intermediates 4-aminomethylindole and 3-indole-AA as sole carbon sources, while exhibiting a robust growth on 3-indole-Ald and 3-indole-CA. UPLC-HRMS analysis during gramine whole cell biotransformation confirmed the transient accumulation of these two intermediates. Therefore, the initial reaction in the proposed pathway likely directly removes dimethylamine to form 3-indole-Ald with the participation of water, and then, generate 3-indole-CA with the participation of water. The aerobic degradation pathway of 3-indole-CA is hypothesized to follow a catechol-mediated metabolic cascade, analogous to the established catabolism of indole-3-acetic acid (IAA) by strain *Arthrobacter* IV [56,57]. Proposed steps include dihydroxylation of the indole ring, subsequent oxidative cleavage and hydrolysis to produce catechol. This intermediate is ultimately channeled into the TCA cycle (Fig. 6B). Genomic analysis in this study identified a gene cluster (gene581-gene592) exhibiting homology to catechol meta-cleavage pathway. Notably, this cluster encodes several oxidoreductase and hydrolase proteins, suggesting their potential roles in the downstream degradation in gramine catabolism by strain NyZ202 (Table S5).

4. Conclusions

This study presents the first investigation into the microbial degradation of barley alkaloids (hordenine or gramine), leading to the isolation and characterization two rhizobacterial strains, NyZ201 and NyZ202, from barley rhizosphere soil. Growth assays revealed their abilities to utilize not only the parent alkaloids (hordenine or gramine), but also downstream catabolic intermediates for growth. Integrated

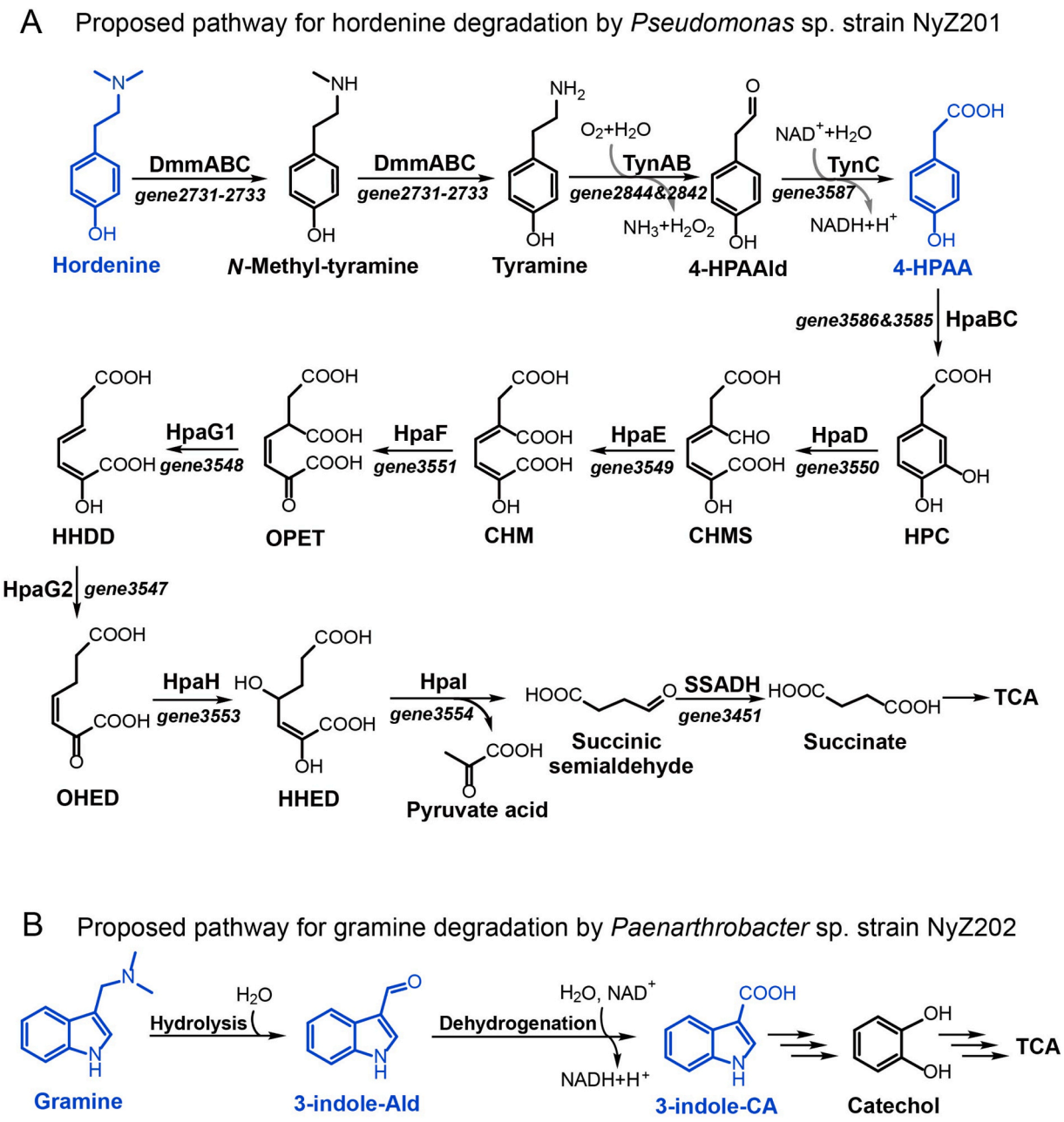

Fig. 6. Proposed aerobic catabolic pathways for hordenine by *Pseudomonas* sp. strain NyZ201 (A) and gramine by *Paenarthrobacter* sp. strain NyZ202 (B). Blue-colored compounds were identified by HPLC and UPLC-HRMS. The substrates and products are: 4-HPAAld (4-hydroxyphenylacetaldehyde); 4-HPAA (4-hydroxyphenylacetate); HPC (3,4-dihydroxyphenylacetate); CHMS (5-carboxymethyl-2-hydroxymuconic semialdehyde); CHM (5-carboxymethyl-2-hydroxymuconic acid); OPET (5-oxo-pent-3-ene-1,2,5-tricarboxylic acid); HHDD (2-hydroxy-hept-2,4-diene-1,7-dioic acid); OHED (2-oxo-hept-3-ene-1,7-dioic acid); HHED (2,4-dihydroxy-hept-2-ene-1,7-dioic acid).

genomic and catabolic intermediates analyses enabled the identification of putative gene clusters associated with hordenine- and gramine-degrading pathways. Bacteria-mediated alkaloids degradation likely plays an essential role in their recycling within the soil environment, and may influence the rhizospheric microbial composition by reducing alkaloid concentrations or releasing degradation intermediates. Moreover, as alkaloids function as plant defensive compounds against phytophagous insects, and the movement of the alkaloids-degrading bacteria or genes into insect gut microbiome may confer them alkaloids resistance via microbial detoxification[58]. Future biochemical characterization of the genetic determinants for hordenine and gramine degradation will reveal the ecologic impacts of bacterial alkaloid degradation. These findings elucidate the microbial mechanisms of alkaloid degradation and provide a foundation for detoxifying phytotoxic alkaloids in agricultural ecosystems.

Environmental implication

Barley-derived alkaloids, hordenine and gramine, poses ecological risks in agricultural soils due to their persistent toxicities. Additionally, gramine has been identified as toxic to ruminants, posing a significant concern in pasture management. Considering their toxicity, they should be regarded as "hazardous materials".

In this study, two bacterial strains were isolated due to their robust catabolic activities in utilizing hordenine and gramine as sole carbon and nitrogen sources, respectively. Through the identification of

metabolic intermediates and genomic analysis, the degradation pathways of these alkaloids were proposed. This discovery offers insights into sustainable strategies for phytotoxic alkaloids detoxification in agricultural systems.

CRediT authorship contribution statement

Ning-Yi Zhou: Writing – review & editing, Writing – original draft, Supervision, Resources, Project administration, Conceptualization. **Yanfei Wu:** Writing – review & editing, Writing – original draft, Methodology, Investigation, Formal analysis, Data curation. **Tao Li:** Writing – review & editing, Writing – original draft, Validation, Supervision, Funding acquisition, Conceptualization.

Declaration of Competing Interest

The authors declare that they have no known competing financial interests or personal relationships that could have appeared to influence the work reported in this paper.

Acknowledgments

This work was supported by grant from the National Key R&D Program of China (2021YFA0910300).

Supporting information

Additional 8 figures and 5 tables with details of degradation products identification, growth experiment and genome information.

Appendix A. Supporting information

Supplementary data associated with this article can be found in the online version at doi:10.1016/j.jhazmat.2025.139299.

Data availability

Data will be made available on request.

References

[1] Kumar, Anjali, S., Korra, T., Thakur, R., Arutselvan, R., Kashyap, A.S., Nehela, Y., et al., 2023. Role of plant secondary metabolites in defence and transcriptional regulation in response to biotic stress. Plant Stress 8, 100154.
[2] Zhou, X., Zhang, J., Khashi, M., u, Rahman, D., Gao, Z., et al., 2023. Dini-Andreote, Interspecific plant interaction via root exudates structures the disease suppressiveness of rhizosphere microbiomes. Mol Plant 16, 849–864.
[3] Günthardt, B.F., Hollender, J., Hungerbühler, K., Scheringer, M., Bucheli, T.D., 2018. Comprehensive toxic plants–phytotoxins database and its application in assessing aquatic micropollution potential. J Agr Food Chem 66, 7577–7588.
[4] Bucheli, T.D., 2014. Phytotoxins: environmental micropollutants of concern? Environ Sci Technol 48, 13027–13033.
[5] Núñez, M.D., Loveira, E.G.L., Domínguez, S.E., Calfayan, L.M., Itria, R.F., Butler, M., 2025. Assessment of nicotine and degradation products in cigarette butts leachates after detoxification by white rot fungi. J Hazard Mater 492, 138059.
[6] Macías, F.A., Oliveros-Bastidas, A., Marín, D., Castellano, D., Simonet, A.M., Molinillo, J.M.G., 2005. Degradation studies on benzoxazinoids.: soil degradation dynamics of (2R)-2-*O*-β-D-Glucopyranosyl-4-hydroxy-(2*H*)- 1,4-benzoxazin-3(4*H*)-one (DIBOA-Glc) and its degradation products, phytotoxic allelochemicals from Gramineae. J Agr Food Chem 53, 554–561.
[7] Thoenen, L., Kreuzer, M., Pestalozzi, C., Florean, M., Mateo, P., Züst, T., et al., 2024. The lactonase BxdA mediates metabolic specialisation of maize root bacteria to benzoxazinoids. Nat Commun 15, 6535.
[8] Abegaz, B.M., Kinfe, H.H., 2019. Secondary metabolites, their structural diversity, bioactivity, and ecological functions: an overview. Phys Sci Rev 4, 20180100.
[9] Liu, D.L., Lovett, J.V., 1993. Biologically active secondary metabolites of barley. I. Developing techniques and assessing allelopathy in barley. J Chem Ecol 19, 2217–2230.
[10] Hoult, A.H.C., Lovett, J.V., 1993. Biologically active secondary metabolites of barley. III. A method for identification and quantification of hordenine and gramine in barley by high-performance liquid-chromatography. J Chem Ecol 19, 2245–2254.
[11] Maver, M., Miras-Moreno, B., Lucini, L., Trevisan, M., Pii, Y., Cesco, S., et al., 2020. New insights in the allelopathic traits of different barley genotypes: middle Eastern and Tibetan wild-relative accessions vs. cultivated modern barley. Plos One 15, e0231976.
[12] K.R, J., Moncef, B.-H., 2009. Allelopathic plants. 19. barley (*Hordeum vulgare* L). Allelopath J 24, 225–242.
[13] Lovett, J.V., Hoult, A.H.C., Christen, O., 1994. Biologically active secondary metabolites of barley.IV. Hordenine production by different barley lines. J Chem Ecol 20, 1945–1954.
[14] Leete, E., Marion, L., 1953. The biogenesis of alkaloids: VII. The formation of hordenine and n-methyltyramine from tyrosine in barley. Can J Chem 31, 126–128.
[15] Schenck, C.A., Maeda, H.A., 2018. Tyrosine biosynthesis, metabolism, and catabolism in plants. Phytochemistry 149, 82–102.
[16] Dias, S.L., Chuang, L., Liu, S., Seligmann, B., Brendel, F.L., Chavez, B.G., et al., 2024. Biosynthesis of the allelopathic alkaloid gramine inbarley by a cryptic oxidative rearrangement. Science 383, 1448–1454.
[17] Grün, S., Frey, M., Gierl, A., 2005. Evolution of the indole alkaloid biosynthesis in the genus *Hordeum*: Distribution of gramine and DIBOA and isolation of the benzoxazinoid biosynthesis genes from *Hordeum lechleri*. Phytochemistry 66, 1264–1272.
[18] Zúñiga, G.E., Salgado, M.S., Corcuera, L.J., 1985. Role of an indole alkaloid in the resistance of barley seedlings to aphids. Phytochemistry 24, 945–947.
[19] Ishiai, S., Kondo, H., Hattori, T., Mikami, M., Aoki, Y., Enoki, S., et al., 2016. Hordenine is responsible for plant defense response through jasmonate-dependent defense pathway. Physiol Mol Plant P 96, 94–100.
[20] Sun, X.Q., Zhang, M.X., Yu, J.Y., Jin, Y., Ling, B., Du, J.P., et al., 2013. Glutathione S-transferase of brown planthoppers (*Nilaparvata lugens*) is essential for their adaptation to gramine-containing host plants. Plos One 8, e64026.
[21] Cai, Q.N., Zhang, Q.W., Cheo, M., 2004. Contribution of indole alkaloids to *Sitobion avenae* (F.) resistance in wheat. J Appl Entomol 128, 517–521.
[22] Matsuo, H., Taniguchi, K., Hiramoto, T., Yamada, T., Ichinose, Y., Toyoda, K., et al., 2001. Gramine increase associated with rapid and transient systemic resistance in barley seedlings induced by mechanical and biological stresses. Plant Cell Physiol 42, 1103–1111.
[23] Zúñiga, G.E., Corcuera, L.J., 1986. Effect of gramine in the resistance of barley seedlings to the aphid *Rhopalosiphum padi*. Entomol Exp Appl 40, 259–262.
[24] Hong, Y., Hu, H.Y., Xie, X., Sakoda, A., Sagehashi, M., Li, F.M., 2009. Gramine-induced growth inhibition, oxidative damage and antioxidant responses in freshwater cyanobacterium. Aquat Toxicol 91, 262–269.
[25] Gallagher, C.H., Koch, J.H., Steel, J.D., Moore, R.M., 1964. Toxicity of Phalaris Tuberosa for Sheep. Nature 204, 542–545.
[26] Hanson, A.D., Traynor, P.L., Ditz, K.M., Reicosky, D.A., 1981. Gramine in Barley Forage - Effects of Genotype and Environment. Crop Sci 21, 726–730.
[27] Lebecque, S., Crowet, J.M., Lins, L., Delory, B.M., du Jardin, P., Fauconnier, M.L., et al., 2018. Interaction between the barley allelochemical compounds gramine and hordenine and artificial lipid bilayers mimicking the plant plasma membrane. Sci Rep 8, 9784.
[28] Maver, M., Trevisan, F., Miras-Moreno, B., Lucini, L., Trevisan, M., Cesco, S., et al., 2022. The interplay between nitrogenated allelochemicals, mineral nutrition and metabolic profile in barley roots. Plant Soil 479, 715–730.
[29] Maver, M., Escudero-Martinez, C., Abbott, J., Morris, J., Hedley, P.E., Mimmo, T., et al., 2021. Applications of the indole-alkaloid gramine modulate the assembly of individual members of the barley rhizosphere microbiota. Peerj 9, e12498.
[30] Liu, Y., Li, J.-J., Li, H.-Y., Deng, S.-M., Jia, A.-Q., 2021. Quorum sensing inhibition of hordenine analogs on *Pseudomonas aeruginosa* and *Serratia marcescens*. Synth Syst Biotechnol 6, 360–368.
[31] Schütz, V., Frindte, K., Cui, J., Zhang, P., Hacquard, S., Schulze-Lefert, P., et al., 2021. Differential impact of plant secondary metabolites on the soil microbiota. Front Microbiol 12, 666010.
[32] Cycon, M., Mrozik, A., Piotrowska-Seget, Z., 2017. Bioaugmentation as a strategy for the remediation of pesticide-polluted soil: a review. Chemosphere 172, 52–71.
[33] Sparnins, V.L., Chapman, P.J., 1976. Catabolism of L-tyrosine by the homoprotocatechuate pathway in gram-positive bacteria. J Bacteriol 127, 362–366.
[34] Arcos, M., Olivera, E.R., Arias, S., Naharro, G., Luengo, J.M., 2010. The 3,4-dihydroxyphenylacetic acid catabolon, a catabolic unit for degradation of biogenic amines tyramine and dopamine in *Pseudomonas putida* U. Environ Microbiol 12, 1684–1704.
[35] Roager, H.M., Licht, T.R., 2018. Microbial tryptophan catabolites in health and disease. Nat Commun 9, 3294.
[36] Ma, Q., Zhang, X., Qu, Y., 2018. Biodegradation and biotransformation of indole: advances and perspectives. Front Microbiol 9, 2625.
[37] Arora, P.K., Sharma, A., Bae, H., 2015. Microbial degradation of indole and its derivatives. J ChemNy, 129159.
[38] Luo, C., He, Y., Chen, Y., 2025. Rhizosphere microbiome regulation: unlocking the potential for plant growth. Curr Res Microb Sci 8, 100322.
[39] Wu, L., Weston, L.A., Zhu, S., Zhou, X., 2023. Editorial: rhizosphere interactions: root exudates and the rhizosphere microbiome. Front Plant Sci 14, 1281010.
[40] Huang, Y.H., Zhou, S.K., Chen, W.J., Zhou, X.F., Chen, S.F., Song, H.R., et al., 2025. Mechanistic insights into D-cyphenothrin biodegradation by *Rhodococcus ruber* Y14 and its potential for bioremediation of pyrethroid-polluted environment. Chem Eng J 506, 160030.
[41] Weisburg, W.G., Barns, S.M., Pelletier, D.A., Lane, D.J., 1991. 16s Ribosomal DNA Amplification for Phylogenetic Study. J Bacteriol 173, 697–703.

[42] Sayers, Eric W., Beck, J., Bolton, Evan E., Brister, J.R., Chan, J., Comeau, Donald C., et al., 2024. Database resources of the national center for biotechnology information. Nucleic Acids Res 52, D33–D43.
[43] Chalita, M., Kim, Y.O., Park, S., Oh, H.-S., Cho, J.H., Moon, J., et al., 2024. EzBioCloud: a genome-driven database and platform for microbiome identification and discovery. Int J Syst Evolut Microbiol 74, 006421.
[44] Tamura, K., Stecher, G., Kumar, S., 2021. MEGA11: molecular evolutionary genetics analysis version 11. Mol Biol Evol 38, 3022–3027.
[45] Buchfink, B., Xie, C., Huson, D.H., 2015. Fast and sensitive protein alignment using DIAMOND. Nat Methods 12, 59–60.
[46] Blin, K., Shaw, S., Steinke, K., Villebro, R., Ziemert, N., Lee, S.Y., et al., 2019. antiSMASH 5.0: updates to the secondary metabolite genome mining pipeline. Nucleic Acids Res 47, W81–W87.
[47] Grant, J.R., Enns, E., Marinier, E., Mandal, A., Herman, E.K., Chen, C.Y., et al., 2023. Proksee: in-depth characterization and visualization of bacterial genomes. Nucleic Acids Res 51, 484–492.
[48] Richter, M., Rosselló-Móra, R., Glöckner, F.O., Peplies, J., 2016. JSpeciesWS: a web server for prokaryotic species circumscription based on pairwise genome comparison. Bioinformatics 32, 929–931.
[49] Malhotra, H., Dhamale, T., Kaur, S., Kasarlawar, S.T., Phale, P.S., 2024. Metabolic engineering of *Pseudomonas bharatica* CSV86^{T} to degrade Carbaryl (1-naphthyl-*N*-methylcarbamate) via the salicylate-catechol route. Microbiol Spectr 12, e0028424.
[50] Iyer, R., Damania, A., 2016. Draft genome sequence of *Pseudomonas putida* CBF10-2, a soil isolate with bioremediation potential in agricultural and industrial environmental settings. Genome Announc 4, e00670-00616.
[51] Luengo, J.M., Olivera, E.R., 2020. Catabolism of biogenic amines in *Pseudomonas* species. Environ Microbiol 22, 1174–1192.
[52] El-Sabeh, A., Mlesnita, A.-M., Munteanu, I.-T., Honceriu, I., Kallabi, F., Boiangiu, R.-S., et al., 2023. Characterisation of the *Paenarthrobacter nicotinovorans* ATCC 49919 genome and identification of several strains harbouring a highly syntenic nic-genes cluster. BMC Genom 24, 536.
[53] Bhattacharyya, A., Mavrodi, O., Bhowmik, N., Weller, D., Thomashow, L., Mavrodi, D., 2023. Bacterial biofilms as an essential component of rhizosphere plant-microbe interactions. Methods Microbiol 3–48.
[54] Singh, K., Chandra, R., Purchase, D., 2022. Unraveling the secrets of rhizobacteria signaling in rhizosphere. RhizosphereNeth 21, 100484.
[55] Diaz, E., Ferrandez, A., Prieto, M.A., Garcia, J.L., 2001. Biodegradation of aromatic compounds by *Escherichia coli*. Microbiol Mol Biol Rev 65, 523–569.
[56] Mino, Y., 1970. Studies on the destruction of indole-3-acetic acid by a species of *Arthrobacter* IV. Decomposition products. Plant Cell Physiol 11, 129–138.
[57] Scott, J.C., Greenhut, I.V., Leveau, J.H.J., 2013. Functional characterization of the bacterial iac genes for degradation of the plant hormone indole-3-acetic acid. J Chem Ecol 39, 942–951.
[58] Zhang, N., Qian, Z.Y., He, J.T., Shen, X.Q., Lei, X.Y., Sun, C., et al., 2024. Gut bacteria of lepidopteran herbivores facilitate digestion of plant toxins. P Natl Acad Sci 121, e2412165121.